REPORT

INVESTIGATION OF THE INFLUENCE OF THE SCATTERING COEFFICIENT ON ACOUSTO-OPTIC MODULATION EFFICIENCY IN TURBID PHANTOMS

Huub Vermeulen

FACULTY OF SCIENCE AND TECHNOLOGY
BIOMEDICAL PHOTONIC IMAGING

EXAMINATION COMMITTEE
Prof. Dr. Ir. Wiendelt Steenbergen
Altaf Hussain (MSc)
Dr. Mireille Claessens

DOCUMENT NUMBER
TNW - S0191841

UNIVERSITY OF TWENTE.

13-07-2012

Abstract

Photo-acoustic imaging (PAI) and acousto-optic imaging (AOI) are two front line biomedical photonic imaging modalities, developed to overcome the issues with deep tissue photonic imaging. A technique to compensate for fluence in photo-acoustic imaging (PAI) with the use of acousto-optic imaging (AOI) was developed by Daoudi et al. [1] The effect of local scattering on these modalities has not been taken into account yet. The objective of this study was therefore to investigate what influence the local scattering coefficient of the medium has on acousto-optic modulation in turbid phantoms. AOI and Pressure contrast imaging (PCI) measurements with self-made and characterized turbid agar gel phantoms were performed and a relation between scattering contrast and AO modulation is investigated. The results show that there is a prominent non-linear relation between scattering coefficient of the medium and AO modulation efficiency for a limited range of reduced scattering coefficient from 2 till 5 cm^{-1}. For higher values the dependence of AO modulation efficiency on scattering coefficient becomes very small or so to speak negligible. However, the results obtained during this research work are qualitative and are yet to be quantified.

Acknowledgement

I would like to acknowledge and extend the utmost gratitude to the following persons who have helped make this study's completion a possibility:

My daily supervisor, Altaf Hussain, for his constant motivation, support and unending patience.

Prof. Dr. Ir. Wiendelt Steenbergen, for the hearty pushes that helped me finish almost on schedule.

Dr. Srirang Manohar for his advice which helped steer this research in the right direction.

All BmPI faculty members and staff for all the little ways in which they have helped me over the past three months.

And last but not least, my family and friends, for their words of encouragement and for putting up with me boring them with subjects far too complicated for small talk.

Table of Contents

1. Introduction 5
   1.1 Motivation 6
   1.2 Research Problem 6
2. Materials and Methods 7
   2.1 Solid turbid agar phantoms 7
   2.2 Preparation of the phantoms 7
   2.3 Measuring the reduced scattering coefficient 8
   2.5 First experiment: Scattering contrast inclusions 10
   2.6 Second experiment: Pressure contrast imaging 11
3. Results 12
   3.1 Reduced scattering coefficient 13
   3.2 Effect of the local scattering coefficient on AO modulation 13
   3.3 Pressure contrast imaging 14
4. Discussion 17
5. Summary and Conclusion 18
6. Outlook 19
7. References 20

1. Introduction

This chapter will feature a brief explanation of the imaging modalities that are central to this research, followed by a motivation for the study and concluding with a statement of the research problem.

Biomedical photonic imaging (BMPI) plays a very important role in the field of biomedical diagnostics and biomedicine. The importance of biomedical imaging in this field stems from the interaction of light with biological tissue, which provides very unique and abundant information about the physiology of tissue and its constituents. One of the biggest challenges in BMPI is imaging deep inside biological tissue, this is a result of strong light scattering inside biological tissue which degrades the imaging resolution and makes pure optical imaging impossible deeper than a few 100 micrometers. Several techniques are being investigated for imaging deep into biological tissue. Photo-acoustic imaging (PAI) and acousto-optic imaging (AOI) are two front line imaging modalities that are being researched to overcome this problem. Both of these modalities combine ultrasound and light, which results in a combination of ultrasonic resolution and optical contrast. [2]

PAI is a modality based on the photoacoustic effect. The photoacoustic effect can be described as the generation of soundwaves by the absorption of photonic energy. When electromagnetic waves are absorbed they are converted to heat; it is a well known fact that, generally, when materials are heated they expand. If the heating occurs rapidly enough the expanding material will produce a wave of pressure, of sound, which can be measured. [3] This is why in PAI, a pulsed laser is used to achieve the necessary heating; ultrasound transducers are used to measure the resulting waves of pressure.

AOI takes its name from the acousto-optic effect. The acousto-optic effect is the modulation of light travelling through ultrasound. The light that has been modulated is referred to as ‘tagged’ light. There are two main mechanisms we are interested in, which one is dominant depends on the optical properties of the medium the ultrasound travels through. When trying to understand these mechanisms it can be instructive to remember that the speed of sound is extremely slow compared to the speed of light; the waves of sound can be approximated to be stationary compared to the light. The end result of this modulation is variation in the intensity of the speckle pattern on the detector.

These mechanisms work by changing the optical phase of photons passing through the ultrasound beam. The first mechanism works as follows: The ultrasound causes the displacement of scattering particles at its frequency, the photons scattering off of these particles experience a different mean free path than they might have otherwise, resulting in a different optical phase upon exiting the medium. [4]

The third mechanism occurs due to the changes in density that are caused by the pressure waves. The density has an effect on the index of refraction, generally speaking the index of refraction increases when the density does. Light travelling through these changed indexes of refraction once again has its travelling time between consecutive scattering events, and thus its optical phase, modulated. [4]

Besides these changes in optical phase, the light also undergoes changes in frequency due to the Doppler Effect, the size of the frequency of the ultrasound. This phenomenon can be exploited to improve the signal to noise ratio in AOI, as will be explained in the materials and methods section.

1.1 Motivation

One of the remaining issues with these modalities is the dependence of the signal on fluence which varies depending on the optical properties of the medium. The fluence is a measure of energy over area, to our knowledge there is no existing method for measuring the local fluence non-invasively. More light in a specific area of the medium means more tagging in case of AOI and more pressure in case of PAI, so both modalities have an increase in signal due to fluence. Absorption acts as a sink for the fluence; in AOI this is visible as a decrease in signal, in PAI however the initial stress distribution is proportional to the local absorbed energy.

This different dependence of signal on fluence and absorption has been used by Daoudi et al. [1] to compensate for the fluence and map the absorption inside phantoms. Eq. (1.1) shows the proportionality of the absorption coefficient to the combined signal of the two modalities.

$$\mu_{a,2} = \frac{1}{\Gamma}\sqrt{\frac{A_2 A_3 \Omega_3}{4\pi}}\sqrt{\frac{P_1}{E_{p,1}E_{p,3}}}\sqrt{\frac{p_{21}p_{32}}{P_{L,123}}} \tag{1.1}$$

Where $\mu_{a,2}$ is a local absorption coefficient, the first square root contains solely instrumental geometrical parameters, the second square root contains excitation parameters and the third square root contains externally measurable quantities. p_{21} and p_{32} are two pressures measured with PAI and $P_{L,123}$ is the signal from an AOI measurement.

1.2 Research Problem

However, eq. (1) does not take into account the influence of local scattering on AO modulation of light inside the tagging volume. The reduced scattering coefficient (μ_s') plays a role in the acousto-optic modulation, so local scattering of the medium might affect the tagging efficiency of AO modulation.

The objective of this study is therefore to investigate what influence the local scattering coefficient of the medium has on acousto-optic modulation in turbid phantoms.

2. Materials and Methods

In this chapter, first the phantoms that were prepared, and then the way they were characterized will be explained. This is followed by a section on the AOI setup, and finished with a description of the performed experiments.

2.1 Solid turbid agar phantoms

In order to experiment in a directed, cheap and safe manner, mediums are created to serve as a substitute for actual tissue. These tissue like media are referred to as phantoms. In order to make proper phantoms for acousto-optics measurements, both the acoustic and optical properties need to be taken into account. For the acoustic properties the density and the speed of sound inside the medium and the elasticity of the medium are of importance. A way to mimic these properties is the use of an agar gel, which, similar to biological tissue, has water as a main constituent.

A gel consisting of 2% agar in water has roughly the same acoustical properties as soft human tissue.[5] For the optical properties substances can be added to the agar gel during the process of making it. The propertie we are interested in is scattering, and to mimic this property intralipid (IL) 20% is used. Intralipid is the brand name for a fat emulsion used for intravenous therapy in humans.

2.2 Preparation of the phantoms

The phantoms are made as follows: first, an amount of demineralized water is measured, and a 2% W/Vol. of agar powder is added. This solution needs to be heated to 95 ˚C, which is the melting point of agar. This is done by heating the solution in a microwave oven for even heating. Then the solution is cooled down to about 60 ˚C, before adding IL. The solution needs to be continually stirred while it is cooling down to achieve a homogeneous texture and to make it free of air bubbles. When it has reached a temperature of 60 ˚C, IL is added and the mixture is continuously stirred till it reaches 40^{o}C and can be poured into its mold. [5]

Fig. 2.1: is an example of such a self-made phantom, in a cylindrical tube.

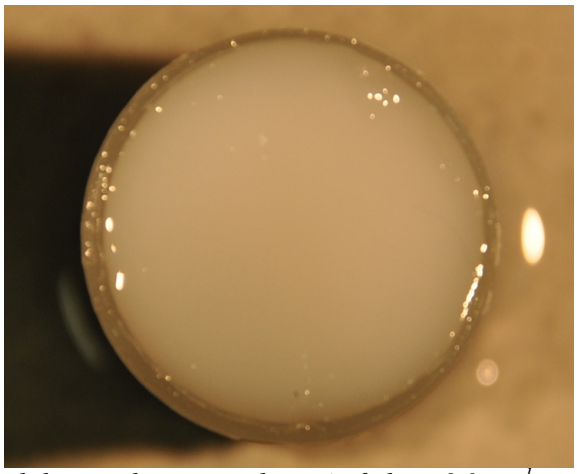

Figure 2.1: *A solid agar phantom with a μ_s' of about 8.9 cm^{-1}, viewed from the top*

2.3 Measuring the reduced scattering coefficient

The μ_s' is a property which actually incorporates two properties; the scattering coefficient and the anisotropy.

$$\mu_s' = \mu_s (1 - g) \quad (2.1)$$

Where μ_s' is the reduced scattering coefficient in cm^{-1}, μ_s is the scattering coefficient in cm^{-1} and g is the dimensionless anisotropy. The scattering coefficient is the inverse of the mean free path, which is the average distance between two scattering events. A scattering event is a collision between, in this case, a photon and a particle. The anisotropy tells us how big the average angle is under which the photons are scattered by such a collision, with 1 being forward, 0 being isotropic scattering and -1 being backwards. It has been shown experimentally in our group that for agar concentration of 2% or higher the anisotropy (g) remains constant and its constant value is 0.9, similar to soft tissue.

So $1/\mu_s'$ gives an approximation of the length of the steps of the random walk diffuse light makes through a medium, more steps generally means a longer path and less certainty about where the light exits.

The μ_s' of the phantoms need to be determined. For this purpose, simple phantoms with intralipid (20%) concentrations ranging from 1% to 10% Vol./Vol. with steps of 1%, and a constant concentration of 2% agar were prepared in Petri dishes with a diameter of 90 mm and a thickness of 10 mm. Therefore from the equation it is clear that any variation in μ_s' is a result of variation in μ_s only.

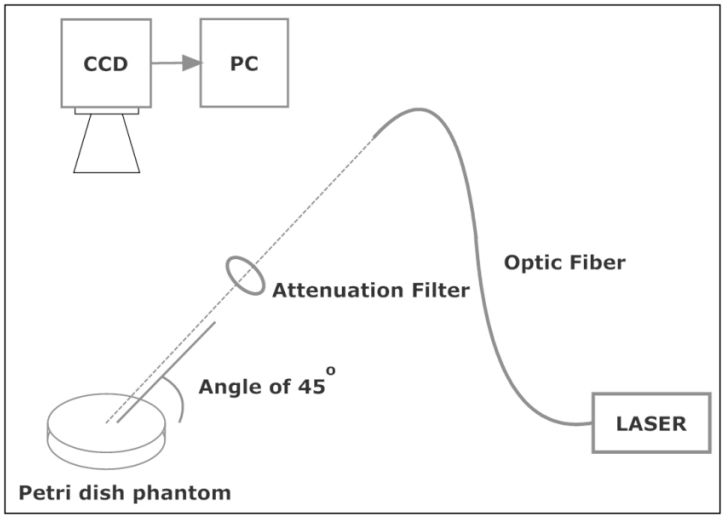

***Figure 2.2**: Schematic of the setup used to determine the μ_s'*

A schematic of the setup of the method we used to determine the μ_s' is shown in Fig. 2.2. Laser light is shone on to a phantom under an angle, and a CCD camera situated directly above the phantom takes images of the result. Light scatters back out of the medium in a diffuse fashion. The center of this diffuse reflectance will appear a certain distance Δx away from the point of incidence; this distance depends on the μ_s' and the index of refraction.

$$\mu_s' = \frac{\sin(\alpha_i)}{n\Delta x} \tag{2.2}$$

Where α_i is the angle of incidence, for which we chose 45 ˚, n is the ratio of the refractive indexes of the air and the medium and Δx is the distance between the point of incidence and the center of the diffuse reflectance. [6]

Three images per phantom are made, one with low laser light, one with high laser light and one entirely dark, as a reference. These images are then analyzed to determine the value of the μ_s', with a matlab algorithm written by Xia et al. [7]

There is one more point that requires addressing; the μ_s' is dependent on the wavelength of the light. The wavelength of the laser used in this setup was 655 nm, which is close to, but not the same as the wavelength of 750 nm of the laser used in the AOI experiments in this study. The transmission scattering coefficient changes with wavelength with $\lambda^{-0.7}$ in the optical window, so the difference is not overly large.

2.4 Acousto-optic tomography setup

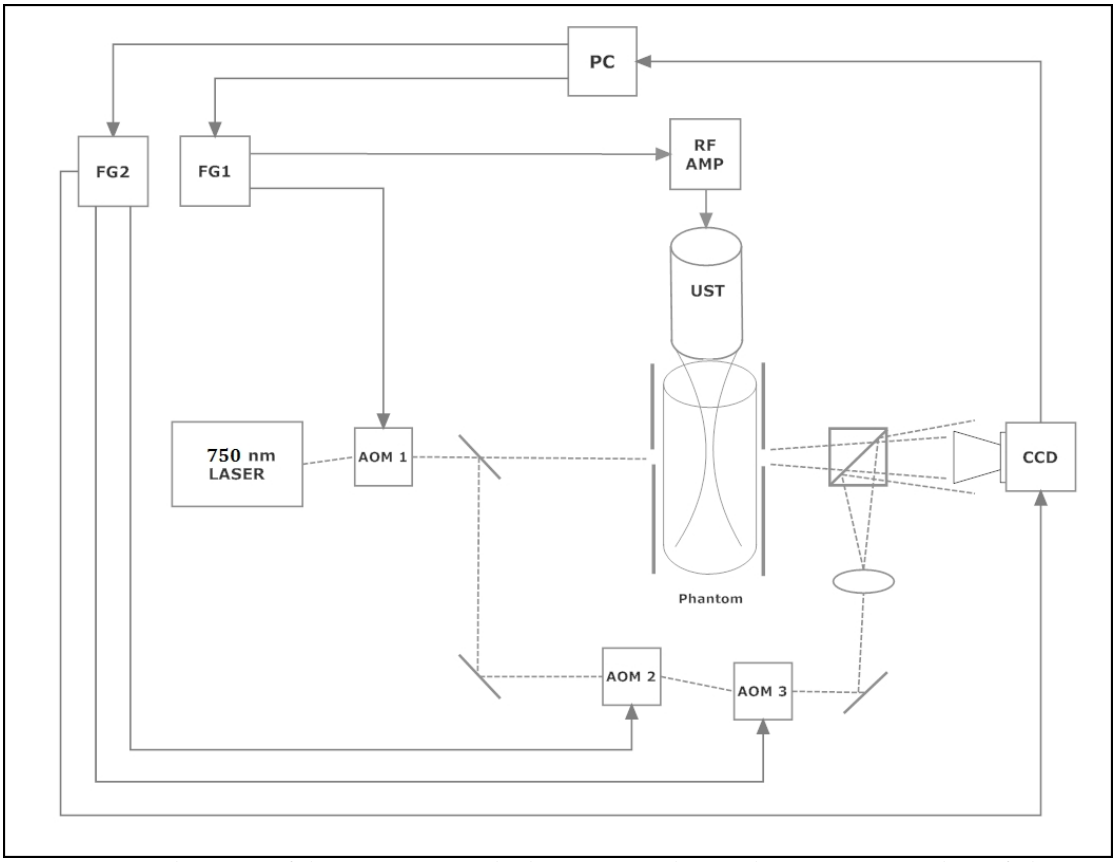

Figure 2.3: *Schematic of the AOT setup. The laser is a Coherent laser group Verdi V6 fed into a Coherent laser group MBR 110, where the laser wavelength is modified to 750nm. FG1 and FG2 are Tektronix afg3102 dual channel function generators. RF AMP is an E&I A075 Power Amplifier. UST is a Panametrics NTD v309 focused 5MHz ultrasound transducer.CCD is a Grey Point Gras 14S5m-c CCD camera. AOM 1 till 3 are NEOS acousto-optic modulators, model number 23080-2-LTD.*

To measure the effect of local scattering coefficient on acousto-optic modulation efficiency we used the experimental set-up shown in Fig. 2.3. The setup is based on a two phase homodyne detection technique, developed by Atlan et al [8]. In essence, the setup consists of an interferometer, with some adaptations.

750 nm laser light is sent through a turbid phantom, which has a mechanically scanning ultrasound transducer above it, sending in waves of focused ultrasound through a layer of water for acoustic coupling. The ultrasound frequency is 5 MHz, and the focused beam of sound is perpendicular to the laser beam. On either side of the phantom holder is an aperture, one for illumination and one to enable detection of the tagged light with the CCD camera. The phantoms used in this study are cylindrical in shape and 20 millimeters in diameter, although other shapes and sizes can also be used in this set-up.

The computer (PC) controls the function generators and the laser, and receives the signal from the camera. Timing is essential in these experiments. The laser and ultrasound need to fire at the right times compared to each other and even the CCD camera needs to be alerted of the incoming information. Interferometry allows for the detection of phase differences in a beam of waves, and the ultrasound modulation changes the optical phase of the laser light, but only a small amount of light is tagged.

As mentioned in the introduction chapter, the Doppler Effect also plays a role in this setup. Due to the Doppler Effect, modulated light gets frequency shifted up or down, with a shift equal to the frequency of the ultrasound. To get a 2 phase interferometric (homodyne) amplification of the tagged light, we use a reference arm with light 5 MHz shifted compared to the sample arm. For this purpose we used AOM2 and AOM3.

$$I_{Homodyne} = 4\sqrt{I_{ref}.I_{tagged}} \tag{2.3}$$

Eq. (2.3) is the equation used to translate the image captured on the CCD camera to the AO signal. $I_{Homodyne}$ is the intensity of the interference pattern on the CCD camera, I_{ref} is the intensity of the light coming from the reference arm of the setup, I_{tagged} is the intensity of the tagged light coming from the phantom.

2.5 First experiment: Scattering contrast inclusions

The first experiment performed in this study used the AOT setup. Cylindrical phantoms were made with a background μ_s' of about 8.9 cm^{-1} (5% IL) and cubical inclusions of 7mm by 7mm by 7mm with a μ_s' of about 20.3 cm^{-1} (10% IL) and about 1.8 cm^{-1} (1% IL), respectively.

Fig. 2.4 is a photo of the phantoms, made during the preparation. The premade inclusions are in place, and once the layer of fluid they are in has solidified, the rest of the tubes will be filled. A third phantom was made of the same shape and background material, but without any inclusions, to serve as a reference for normalization to overcome fluence variations.

A line scan was made through the phantoms, along the optical axis. The scan spans 12 of the 20 mms of the phantoms diameter, in the middle between the two apertures with a step size of 0.5 mm, providing 25 data points. Data is stored for different depths of the ultrasound pulse inside the phantom, with the ultrasound focus at the same depth as the middle of the illumination and detection apertures. These measurements were done for all three phantoms in the exact same way, without changing anything in the setup or alignment besides the phantom.

Figure 2.4: *Unfinished phantoms, to the left with a high μ_s' inclusion, to the right with a low μ_s' inclusion.*

2.6 Second experiment: Pressure contrast imaging

A second experiment was performed with new phantoms. These phantoms, as shown in Fig. 2.5, were of a simpler nature. The same cylindrical shape, but divided into two layers with a different μ_s'. Ten phantoms were made in total, maintaining a μ_s' of 8.9 cm^{-1} in one half and varying the μ_s' in the other half of the phantom from 1.8 till 20.3 cm^{-1}. The phantoms were all placed with the 'background' layer with a μ_s' of 8.9 cm^{-1} on the side where the laser enters the phantom.

Lai et al. [9] developed a new modality dubbed pressure contrast imaging (PCI). Its function is to enhance and even quantify scattering contrast. It is done in the following manner: The phantoms were all measured in two ways, at two different pressures at the ultrasound focus. The higher pressure was as high as 1.2 MPa whereas the lower pressure was as low as 300 KPa. The AO signal at higher pressure was divided by the AO signal at lower pressure to compensate for the fluence variation inside the sample and to enhance the scattering contrast; a higher μ_s' will result in a bigger difference between the higher and lower pressure measurements.

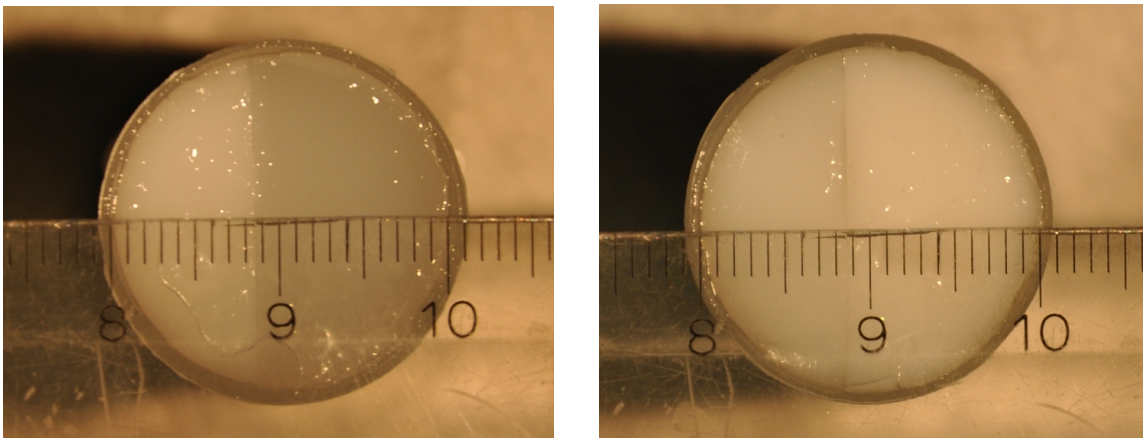

Figure 2.5: *Two phantoms out of the series of ten. To the left the lowest μ_s' phantom, to the right the highest μ_s' phantom.*

3. Results

This chapter will open with the results from the μ_s' measurements. Following up will be the first experiment, with scattering contrast inclusions. It will close with the second experiment, of pressure contrast imaging.

3.1 Reduced scattering coefficient

The μ_s' of 10 phantoms was measured using an oblique angle diffuse reflectance setup. The phantoms were prepared with a fixed agar concentration of 2% W/Vol. and varying Intralipid (20%) concentrations going from 1% till 10% Vol./Vol. The procedure of measuring the μ_s' is described in detail in section 2.3. A matlab algorithm written by Xia Wenfeng was used to calculate the μ_s' from 3 images taken with a CCD camera at different attenuation settings of the illumination beam.

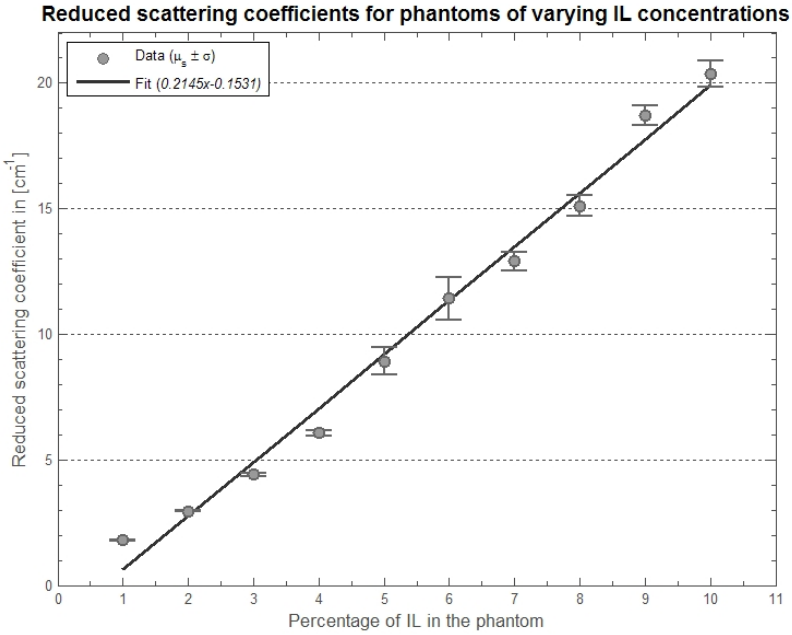

Figure 3.1: *Results of the μ_s' measurements*

The results of the μ_s' measurements for all phantoms are shown in Fig. 3.1. Along the horizontal axis of Fig. 3.1 is the concentration of IL in the phantoms and the vertical axis shows the measured values of the μ_s'. The error bars are the standard deviation of 4 independent measurements done on each phantom. The solid line represents a linear fit that has been applied to the results, which shows a linear relation between IL concentration and μ_s'. Eq. (5) is the linear fit applied to the results, with y being the μ_s' and x being the volume percent of Intralipid (20%) in the agar gel.

$$y = 0.2145x - 0.1531 \qquad (3.1)$$

The μ_s's of these phantoms range from about 1.8 cm^{-1} to about 20.3 cm^{-1}. An approximate average μ_s' for healthy breast tissue is about 9.7 ± 2.2 cm^{-1}, and for breast tumor tissue about 10.8 ± 1.8 cm^{-1}. [10]

3.2 Effect of the local scattering coefficient on AO modulation

To study the effect of the μ_s on AO modulation, AO imaging was performed on three phantoms, all with a background with a μ_s' of 8.9 cm^{-1}. The first phantom with an inclusion of μ_s' of 1.8 cm^{-1}, the second phantom with an inclusion with a μ_s' of 20.3 cm^{-1} and the third phantom without any inclusion. The measurement of these μ_s's is described above; the preparation of these phantoms is described in materials and methods sections 2.2 and 2.5.

The AO imaging was performed with the homodyne detection setup described in section 2.4 of the materials and methods section. The phantoms were placed in a sample holder and a US transducer mechanically scanned 12 mm over the center of the phantom in steps of 0.5 mm along the optical axis from the detection window to the illumination window. The acousto-optic signals of such a line scan for both phantoms with inclusions are shown in Fig. 3.2.

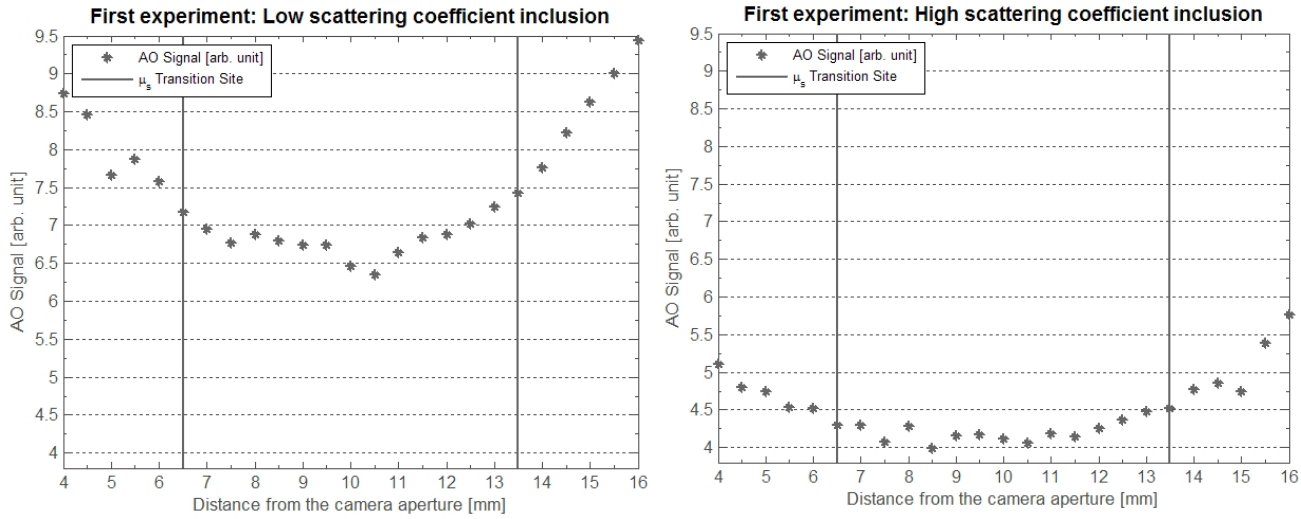

Figure 3.2 : *AO signal line scans through the phantoms with scattering contrast inclusions. On the left, data from the phantom with an inclusion with a μ_s' of approximately 1.8 cm^{-1}. On the right, data from the phantom with an inclusion with a μ_s' of approximately 20.3 cm^{-1}. The vertical lines indicate the edges of the inclusion.*

The results of the AOI measurements for both phantoms with inclusions are shown in Fig. 3.2. Along the horizontal axis of Fig. 3.2 is the distance along the optical axis from the detection window and the vertical axis shows the measured values of the AO signal. The data points are the average value of 4 independent measurements done on each phantom. The vertical lines indicate the edges of the inclusion.

The AO signal of this line scan has a parabolic shape and it would look like the famous banana shape in a 2d or 3d scan [11], which is more prominently a result of the fluence variation inside the scattering medium. The effect we are trying to observe here is a sudden drop or increase in the AO signal at the boundaries of the inclusion due to the sudden change in scattering coefficient. This sudden drop or increase in signal is expected at the boundaries of our inclusions if the AO modulation efficiency is strongly dependent on the local scattering coefficient, since the AO signal due to fluence variation is supposed to have a smooth gradient even close to the boundaries of such inclusions.

Results in fig. 3.2 show, that we do not see a very clear drop or increase in AO signal at the boundaries of the inclusions with contrasting scattering coefficient. This could mean that the influence of the μ_s' variation created in our phantoms is small and is therefore buried under the effect of fluence variation.

In order to verify our results, which show very little dependence of AO signal on local μ_s' another method to see μ_s' contrast in these phantoms was used. This method, proposed by Lai et al [9], is called acousto-optic pressure contrast imaging (PCI) and it was used to measure the μ_s' inside of the turbid media with acousto-optics.

3.3 Pressure contrast imaging

In this pressure contrast imaging experiment a turbid medium with two sections, each with a different μ_s', is subjected to two different values of pressure (P_{Low} and P_{high}) at the US focus and the corresponding AO signals are measured. Then, to see the scattering coefficient contrast in the medium, the ratio $AO_{signal}(P_{High})/ AO_{signal}(P_{Low})$ is calculated. With this method the effect of the μ_s' on the AO signal gets amplified, this amplification factor is proportional to the ΔP and is independent of fluence variations.

The phantoms are again cylindrical, with a diameter of 20 mm. The front halves of the phantoms are all made of the same agar gel with a μ_s' of 8.9 cm^{-1}, the other halves have μ_s's ranging from approximately 1.8 cm^{-1} to 20.3 cm^{-1}.

The PCI was performed with the same homodyne detection setup, described in section 2.4 of the materials and methods section, as the AO imaging in the previous section. The phantoms were placed in a sample holder and a US transducer mechanically scanned 14 mm over the center of the phantom in steps of 0.5 mm along the optical axis from the detection window to the illumination window.

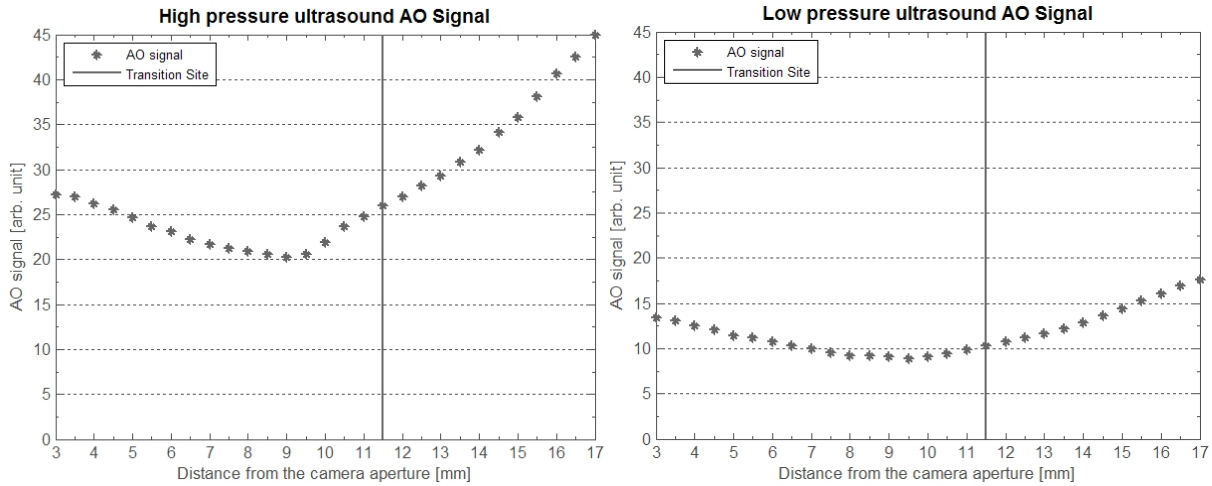

Figure 3.3: *Data from the line scan through the phantom in Fig. 3.4. this particular phantom has the background layer with a μ_s' of approximately 8.9 cm^{-1} and another layer with a μ_s' of 1.8 cm^{-1}. On the left, data from the high pressure AO signal measurement. On the right, data from the low pressure AO signal measurement. The vertical line indicates the transition between the two layers of phantom with different μ_s's.*

The results for both of the PCI measurements for one of the ten phantoms are shown in Fig. 3.3. The phantom used in this measurement is shown in Fig. 3.4. Along the horizontal axis of Fig. 3.3 is the distance along the optical axis from the detection window and the vertical axis shows the measured values of the AO signal. The data points are the average of 4 independent measurements done on each phantom. The vertical line indicates the transition from the first layer into the other.

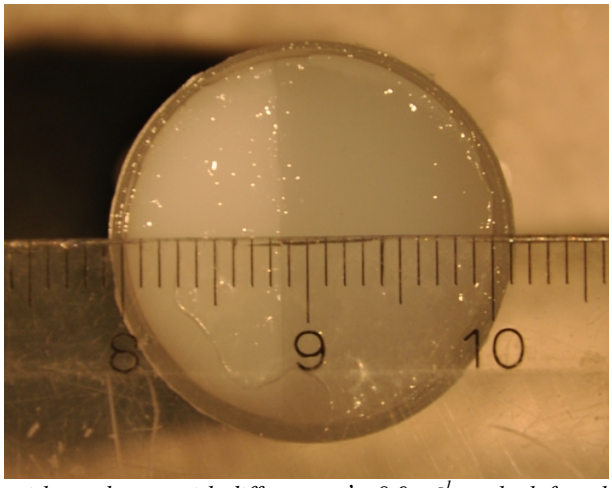

Fig. 3.4: *A phantom with two layers with different μ_s's. 8.9cm^{-1} on the left and 1.8 cm^{-1} on the right.*

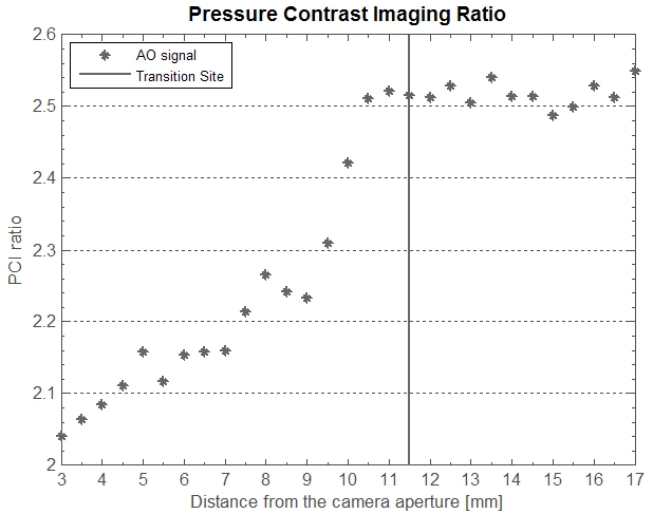

Figure 3.5: *PCI Ratios taken from the two line scans shown in Fig 3.3, made over the phantom in Fig. 3.4. The vertical line indicates the transition between the two layers of phantom with different μ_s's.*

Fig. 3.5 shows the ratio between the high and low pressure data in Fig. 3.3, taken as described at the top of this section. The phantom used in this measurement is shown in Fig. 3.4. Along the horizontal axis of Fig. 3.3 is the distance along the optical axis from the detection window and the vertical axis shows the dimensionless PCI ratio. The vertical line indicates the transition from the first layer into the other.

The contrast between the areas with different μ_s' has now been sufficiently enhanced to be visible.

The next step in this PCI experiment is to take a second ratio. The phantoms have two sections with each a different μ_s' and a transition in between. For this ratio, data points are taken from the PCI ratio plot like the one in Fig. 3.5. Five points from the background layer, $\mu_s'_{bg,}$ and five points from the varying layer $\mu_s'_{var}$. The points from the background layer are divided over the points of the varying layer to get a scattering contrast ratio: $PCI_{ratio}(\mu_s'_{bg})$/ $PCI_{ratio}(\mu_s'_{var})$. The acquired ratio gives a measure of the scattering contrast in the phantom.

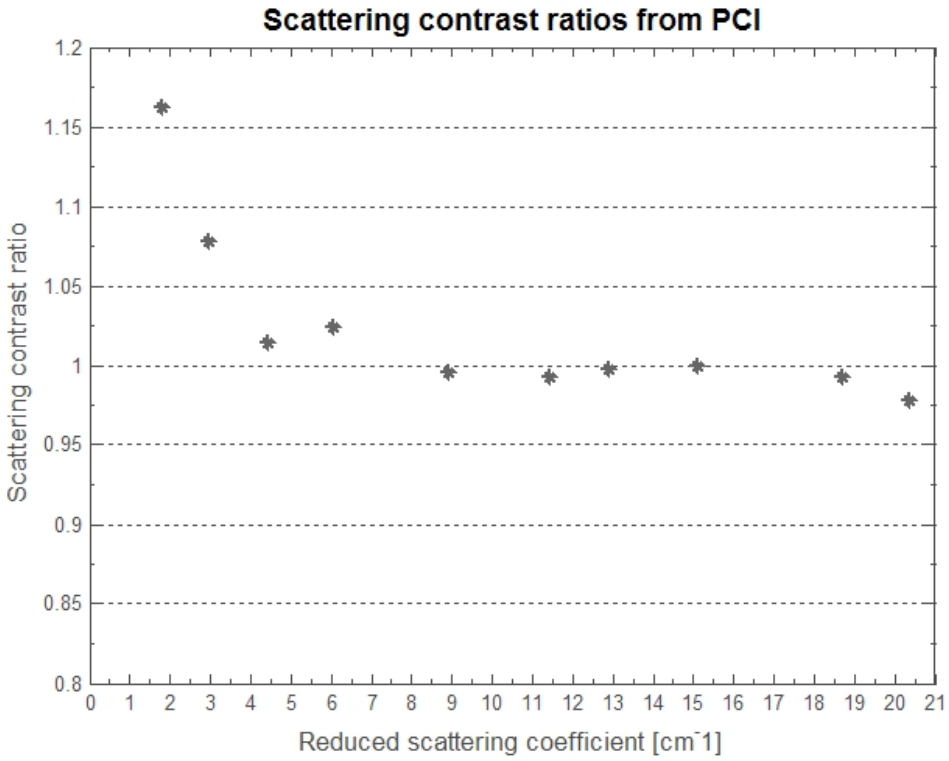

Figure 3.6: *Scattering contrast ratios taken from all of the ten used phantoms.*

Fig. 3.6 shows the scattering contrast ratios for all of the ten used phantoms. Along the horizontal axis of Fig. 3.6 is the $\mu_s'_{var}$ of the phantoms and the vertical axis shows the associated dimensionless scattering contrast ratio.

Since these ratios are taken compared to the $\mu_s'_{bg}$ which is always 8.9 cm^{-1}, we expect the ratios to approach 1 as the $\mu_s'_{var}$ approaches 8.9 cm^{-1}. The further the $\mu_s'_{var}$ lies from that point, the larger we expect the scattering contrast ratio to be.

There appears to be an inverse relation between $\mu_s'_{var}$ and the amount of signal. The inverse relation does not appear to be linear. From the values of μ_s' tested, the scattering contrast caused by a change in AO modulation is greatest for the lowest value of μ_s'. The range of $\mu_s'_{var}$ from 2 till 5 cm^{-1} shows the contrast most clearly, the higher the μ_s' go, the less visible the contrast becomes.

4. Discussion

A technique to compensate for fluence in photo-acoustic imaging (PAI) with the use of acousto-optic imaging (AOI) was developed by Daoudi et al. [1] resulting in Eq. (1.1), an equation linking the local absorption coefficient $\mu_{a,2}$ to externally measurable quantities. The effect of the reduced scattering coefficient (μ_s') on these measurable quantities was then questioned.

In order to study this effect in the case of AOI, phantoms were made and characterized. The amount of Intralipid (20%) in 2% agar gel phantoms was found to linearly correspond to the μ_s' of the phantom. Since the anisotropy (g) remains the same for all these phantoms, it also linearly corresponds to the μ_s of the phantom.

AO line scans were performed through three phantoms with a background layer with a μ_s' of approximately 8.9 cm^{-1}, two of which had an inclusion with a μ_s' of 1.8 cm^{-1} and 20.3 cm^{-1} respectively. The effect of the local scattering contrast on AO modulation was unclear, due to fluence variations inside the phantom caused by the scattering contrast.

Pressure contrast imaging (PCI), as developed by Lai et al. [9], was then performed in order to compensate for the fluence and enhance the μ_s' contrast. These PCI measurements were performed on a new set of ten phantoms. These phantoms all had a background layer with a μ_s' of approximately 8.9 cm^{-1}, and a second layer with a constant μ_s', ranging from 1.8 to 20.3 cm^{-1}.

With the PCI experiment, an inverse relation between reduced scattering coefficient and AO modulation was found. This relation does not appear to be linear. From the values of μ_s' tested, the scattering contrast caused by a change in AO modulation is greatest for the lowest value of μ_s'. The range of $\mu_s'_{var}$ from 2 till 5 cm^{-1} shows the contrast most clearly, the higher the μ_s' goes, the less visible the contrast becomes.

These findings seem to be consistent with the findings of Lai et al. [9] who developed the PCI modality. Their measurements showed that the decrease in AO signal caused by the increase in reduced scattering coefficient rapidly weakens as the reduced scattering coefficient goes from 2 cm^{-1} to 4 cm^{-1}.

Another study explained the mechanism behind this inverse relation. [12] For the amount of modulation of light regarding changes in the reduced scattering coefficient, three terms come in to play:

Firstly the contribution from refractive index changes, which decreases rapidly at first with an increase in scattering. Secondly the contribution from displacement of optical scatterers, which increases rapidly at first when the scattering increases. And finally the anticorrelation between these two mechanisms, which is always negative. Together they result in a sharp decline in modulation, which levels out into an almost linear continuing decrease.

The problem is that this inverse relation has not been quantified yet. The ratios found between the signal levels depend not only on the scattering coefficient, but also on the difference in ultrasound pressure in the PCI measurement.

5. Summary and Conclusion

Photo-acoustic imaging (PAI) and acousto-optic imaging (AOI) are two front line biomedical photonic imaging modalities, developed to overcome the issues with deep tissue photonic imaging. They combine ultrasound and laser light to achieve a combination of ultrasonic resolution and optical contrast.

A technique to compensate for fluence in photo-acoustic imaging (PAI) with the use of acousto-optic imaging (AOI) was developed by Daoudi et al. [1] resulting in Eq. (1.1), an equation linking the local absorption coefficient $\mu_{a,2}$ to externally measurable quantities. These externally measurable quantities may have a dependency on the local scattering coefficient (μ_s). The objective of this study was therefore to investigate what influence the local scattering coefficient of the medium has on acousto-optic modulation in turbid phantoms.

Turbid phantoms were prepared, and characterized with a technique developed by Wang et al. [6] and a matlab algorithm written by Xia et al. [7]. The amount of Intralipid (20%) in 2% agar gel phantoms was found to linearly correspond to the μ_s' of the phantom. Since the anisotropy (g) remains the same for all these phantoms, it also linearly corresponds to the μ_s of the phantom.

An AOI experiment was performed with a setup based on a technique developed by Atlan et al [8]. AOI line scans were made through three phantoms with a background layer with a μ_s' of approximately 8.9 cm^{-1}, two of which had an inclusion with a μ_s' of 1.8 cm^{-1} and 20.3 cm^{-1} respectively. The effect of the local scattering contrast on AO modulation was unclear, due to fluence variations inside the phantom caused by the scattering contrast.

Pressure contrast imaging (PCI), as developed by Lai et al. [9], was then performed with the same AOI setup in order to enhance the μ_s' contrast and compensate for the fluence variations caused by said contrast. These PCI measurements were performed on a new set of ten turbid agar gel phantoms. These phantoms all had a background layer with a μ_s' of approximately 8.9 cm^{-1}, and a second layer with a constant μ_s', ranging from 1.8 to 20.3 cm^{-1}.

With the PCI experiment, an inverse relation between reduced scattering coefficient and AO modulation was found. The inverse relation does not appear to be linear. From the values of μ_s' tested, the scattering contrast caused by a change in AO modulation is greatest for the lowest value of μ_s'. The range of $\mu_s'_{var}$ from 2 till 5 cm^{-1} shows the contrast most clearly, the higher the μ_s' goes, the less visible the contrast becomes. These findings seem to be consistent with the findings of Lai et al. [9] who developed the PCI modality and another study by Kothapalli et al. [12] which explains the mechanisms behind this inverse relation.

6. Outlook

In order to improve the measurements of the effect of the reduced scattering coefficient on AO modulation, I would make the following recommendations:

Attempt to reduce the noise. AOI suffers from high noise levels, caused by a great number of outside factors. Vibrations through the floor from people who walk by, pretty big changes in temperature in the lab, dust in the air landing on optics and samples and even the emergency lighting switching on and off for no apparent reason. In an ideal situation, the experiments would be performed in an entirely closed off environment. This is too much to ask for of course, but some improvements may still be made.

The phantoms are also a source of some differences in results between separate measurements as well. The two layered approach has its uses, but the separate layers do not stick to each other, which could result in water, air or even foreign material getting inside the phantom itself. Phantoms with inclusions are more difficult to properly make, but do not suffer from these issues. For the proper making of square or beam shaped inclusions, a mold would be most useful.

Another possible issue is the ultrasound beam hitting the edges of the tube. Slightly larger phantoms suffer from lower signal, but the ultrasound would pass through cleaner. It might be a good idea to test the propagation of ultrasound with a needle hydrophone through some phantom holders filled with bare phantoms. It could also serve as a test of the material at the bottom of the phantoms which is supposed to absorb the ultrasound.

The real problem that has not yet been overcome in this study, is that the effects of fluence variation due to scattering contrast and change in AO modulation due to scattering contrast are superimposed and need to be separated to get a truly quantified measurement of the latter. I would propose that a study be started to find a way to have two phantoms with the same fluence in a certain area of the phantom, but different scattering coefficients. This need not even be the same area in both phantoms, as long as it's at the same height and far enough away from any edges. This might be achieved by a combination of scattering and absorption, in both simulations and in real phantoms.

7. References

1. Daoudi, K., et al., *Correcting photoacoustic signals for fluence variations using acousto-optic modulation.* OpEx, 2012. **20**(13).
2. Wang, L.V. and others, *Ultrasound-mediated biophotonic imaging: a review of acousto-optical tomography and photo-acoustic tomography.* Disease Markers, 2003. **19**(2-3): p. 123-138.
3. Haisch, C. and R. Niessner, *Light and sound-Photoacoustic spectroscopy.* spectrosc eur, 2002. **14**(5): p. 10-15.
4. Wang, L., *Mechanisms of ultrasonic modulation of multiply scattered coherent light*, in *Biomedical Topical Meeting*2002.
5. Cubeddu, R., et al., *A solid tissue phantom for photon migration studies.* Physics in medicine and biology, 1997. **42**: p. 1971.
6. Wang, L. and S.L. Jacques, *Use of a laser beam with an oblique angle of incidence to measure the reduced scattering coefficient of a turbid medium.* Applied optics, 1995. **34**(13): p. 2362-2366.
7. Xia, W., et al., *Poly(vinyl alcohol) gels as photoacoustic breast phantoms revisited.* J Biomed Opt, 2011. **16**(7): p. 075002.
8. Atlan, M., et al., *Pulsed acousto-optic imaging in dynamic scattering media with heterodyne parallel speckle detection.* Optics letters, 2005. **30**(11): p. 1360-1362.
9. Lai, P., R.A. Roy, and T.W. Murray, *Sensing the optical properties of diffusive media by acousto-optic pressure contrast imaging*, in *Proceedings of SPIE*2009. p. 71771G.
10. Garofalakis, A., et al., *Optical characterization of thin female breast biopsies based on the reduced scattering coefficient.* Phys Med Biol, 2005. **50**(11): p. 2583-96.
11. Lev, A. and B. Sfez, *Pulsed ultrasound-modulated light tomography.* Optics letters, 2003. **28**(17): p. 1549-1551.
12. Kothapalli, S.R., et al., *Imaging of optical scattering contrast using ultrasound-modulated optical tomography*, in *Proc. SPIE*2008. p. 68561p.